Surface Science 604 (2010) 1833–1839

Contents lists available at ScienceDirect

Surface Science

journal homepage: www.elsevier.com/ locate/susc

Spin-asymmetry in elastic scattering of low-energy electrons from ultrathin Au films on W(110)

S.N. Samarin [a,*], J.F. Williams [a], O.M. Artamonov [b], J. Henk [c], R. Feder [d]

[a] The University of Western Australia, Perth WA 6009, Australia
[b] Research Institute of Physics, St. Petersburg University, St. Petersburg 199034, Russia
[c] Max-Planck-Institut für Mikrostrukturphysik, Weinberg 2, D-06120 Halle (Saale), Germany
[d] Theoretische Festkörperphysik, Universität Duisburg-Essen, D-47048 Duisburg, Germany

ARTICLE INFO

Article history:
Received 27 April 2010
Accepted 9 July 2010
Available online 23 July 2010

ABSTRACT

We present joint experimental and theoretical results on the elastic scattering of spin-polarized electrons from an epitaxial Au film on a W(110) substrate in the energy range from 8 eV to 27 eV. A time-of-flight technique with a position-sensitive detector is applied to measure secondary emission spectra for spin-up and spin-down primary electrons in a specular geometry. The spin-asymmetry of coherently scattered electrons is obtained by selecting the diffraction spot on the detector. Regions of large asymmetries – with a maximum of about −60 % – are identified for electron energies of about 14 eV. Relativistic multiple-scattering calculations produce spin-orbit-induced asymmetries which are in agreement with their experimental counterparts. They further reveal that large asymmetries are associated with high intensities. This offers the possibility of an efficient new spin polarimeter with a figure of merit of about $1.5 \cdot 10^{-2}$.

1. Introduction

The scattering of spin-polarized electrons from a Au surface – a text-book example for spin–orbit interaction in a large *Z* material [1–3] – has been extensively studied in the past. The spin dependence is in particular exploited in spin-detecting devices. For example, the scattering of high-energy electrons from a Au foil is a key-element in a classical Mott spin-detector [4]. However, both the spin-asymmetry and the intensity depend strongly on the kinetic energy and the escape angles of the reflected electrons. Thus, for highly efficient spin detectors, the knowledge of 'hot regions' with a large figure of merit – that is the product of intensity and squared spin-asymmetry – is essential. Although in previous investigations, regions with a sizable figure of merit have been found for various surfaces [5,6 and reference therein] there is still a considerable *terra incognita.* We report in this paper on a joint experimental and theoretical investigation, which reveals two so far unknown regions with a large figure of merit.

Our study was motivated by the pioneering theoretical work by R. Feder [7] on spin-polarized Low-Energy Electron Diffraction (SPLEED) from low-index surfaces of Pt and Au. In that work, the calculated polarization of diffracted beams showed a few regions of incident angle and primary energy in which intensity maxima were correlated with polarization maxima, resulting in a favorable figure of merit. A further exploration within a kinematic theory predicted two areas in the low-energy range (primary energy less than 30 eV) where one can expect a highly polarized diffracted beam: one at polar angle $\theta > 50°$ and energy around 25 eV, another at θ around 25−30° and energy below 20 eV (Fig. 4 in [7]). To the best of our knowledge there are no SPLEED measurements on Au(111) in the range of energies below 25 eV, thus calling for a joint experimental and state-of-the-art theoretical investigation.

The identification of regions with a large figure of merit is essential in electron-correlation spectroscopies, for example in (γ, 2e). Struggling with marginal count rates, a spin-polarized final state [that is the time-reversed SPLEED state in (γ, 2e)] is highly desirable. Within this respect, Au(111) and Au/W(110) are of particular interest, since the electron correlations in surface states lend themselves to support for fundamental investigations of correlation effects [8]. The *L*-gap surface state on Au(111) is intrinsically spin-split by the Rashba spin–orbit coupling [9–13], thus allowing to study the spin dependence of the exchange-correlation hole.

Instead of a Au(111) single crystal we used a Au film on W(110), due to its attractive features: (i) easy preparation and (ii) stability in vacuum (low rate of contamination). Au films grow layer-by-layer on W(110) and form an epitaxial but incommensurate layer with (111) orientation [14]. We applied the same methods as in our SPLEED investigation of W(110) [15], focusing on the spin-asymmetry of elastically and specularly scattered electrons in the energy range from 8 eV to 27 eV.

The experiments are accompanied by state-of-the-art relativistic SPLEED calculations for semi-infinite Au(111). Since the spin-asymmetry of elastically scattered low-energy electrons is very sensitive to the

* Corresponding author.
E-mail address: samar@physics.uwa.edu.au (S.N. Samarin).

0039-6028/$ – see front matter © 2010 Elsevier B.V. All rights reserved.
doi:10.1016/j.susc.2010.07.009

details of the potential, we employ the same ingredients as used in our successful studies on photoelectron spectroscopy from Rashba-split surface states [16].

The paper is organized as follows. Experimental and theoretical aspects are described in Sections II and III, respectively. Our measured and calculated results are presented and discussed in Section IV. Conclusions, in particular with regard to a potential new spin polarimeter, are drawn in Section V.

2. Experimental

The experiments were performed in UHV conditions with the base pressure in the 10^{-11} Torr range. The substrate W(110) crystal was mounted on a rotatable manipulator in such a way that the $[1\bar{1}0]$ direction was along the rotational axis and perpendicular to the scattering plane that contains the normal to the sample surface and the detector (Fig. 1).

The substrate was cleaned in a vacuum prior to gold deposition using a standard procedure [17] including oxygen treatment at 10^{-7} Torr oxygen pressure and 1400 K sample temperature followed by a few high-temperature flashes up to 2300 K. The cleanliness of the surface was monitored by Auger Electron Spectroscopy and Low-Energy Electron Diffraction as well as by two-electron coincidence spectroscopy, which is very sensitive to the oxygen presence [18]. The gold film was deposited onto the W(110) substrate at room temperature. It was evaporated from a small piece of gold wire melted on a V-shaped tungsten filament heated resistively. The layer-by-layer growth of such a film was confirmed by MEED oscillations [19]. The quality of the film was demonstrated by observing quantum-well states in such a layer of gold using photoelectron spectroscopy [20]. The 3÷4 ML thickness of the gold layer in our experiment was estimated using Auger peak intensity as a function of deposition time as well as LEED technique and comparison with the previous LEED study of the epitaxy of gold on (110) tungsten [14].

The angle between the incident electron beam and the axis of the detector, as shown in Fig. 1, is 50°. The angle of incidence can be changed by rotating the sample around a vertical axis. We used a time-of-flight technique for electron energy measurements [21]. The incident electron beam is pulsed with a pulse width less than 1 ns to have a reference point on a time scale. Scattered and ejected electrons

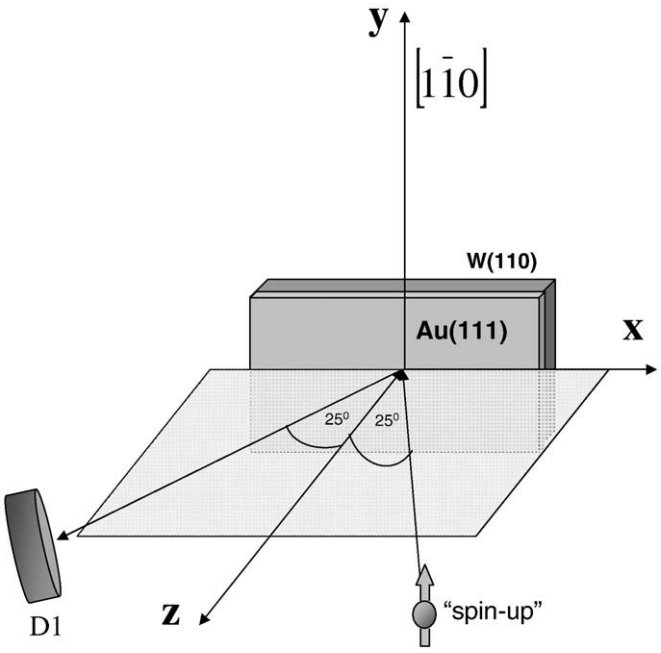

Fig. 1. Experimental geometry.

are detected by a position-sensitive detector based on 75 mm diameter micro-channel plates. The flight distance from the sample to the center of the detector is 126 mm. Position sensitivity of the detector allows the flight distance correction for electrons arriving at different locations on the detector.

The energy resolution of this technique depends on the electron energy and is better for slow electrons than for fast. It can be estimated by the half-width of the elastic maximum, which is 0.5 eV at 14 eV. The spin-polarized electron beam originates from photoemission from a strained GaAs crystal activated by Cs and oxygen adsorption [22]. Photoelectrons excited by circularly polarized light from a diode laser with the wavelength 836 nm are initially longitudinally polarized. They pass through a 90° deflector such that the emergent beam is now transversely polarized. The polarization P of the electron beam is measured in a separate experiment and is estimated to be (66 ± 2) %. It can be reversed from P to $-P$ by changing the sense of circular polarization of the laser light incident on the GaAs photo-cathode. For a given primary energy and fixed experimental geometry the energy distribution curves of secondary electrons are measured for the spin-up (I^{u}) and spin-down (I^{d}) polarization of the incident beam and then the spin-asymmetry is calculated as $A_{exp}=(I^{u}-I^{d})\,/\,(I^{u}+I^{d})$. To take into account the finite polarization P of the incident beam the experimental asymmetry is normalized to the polarization of the beam: $A=A_{exp}/P$. To avoid the influence of the incident electron current drift or the sample surface contamination on the spin-asymmetry during the measurements the polarization of the beam was reversed every 5 s.

We measured the intensity asymmetry of electrons elastically scattered from the sample under diffraction conditions in specular geometry ((00) diffraction beam) for primary electrons with energy from 8 eV to 27 eV. The energy distributions of inelastically scattered electrons were also measured.

The position sensitivity of the detector is used to select only those electrons that scattered coherently and formed a diffraction pattern. Fig. 2a represents an image of the (00) diffraction pattern on the detector in a logarithmic intensity gray scale for $\alpha=\beta=25°$ and primary energy 14 eV. The white circle shows the selected area (inside the circle), which we can assign to the diffraction spot. It means we can choose effectively the acceptance angle of detection by selecting a certain area on the detector. Fig. 2b and c shows the asymmetries of secondary emission spectra measured inside and outside the selection circle for specular geometry and 14 eV primary energy. For both selections, outside and inside of the white circle of Fig. 2, the secondary emission spectrum contains an elastic maximum. It indicates that the gold film is not a perfect crystal and there is a substantial number of elastically scattered electrons outside the diffraction beam that are scattered incoherently. In addition, the incident electron beam is not perfectly paraxial (the beam is divergent).

We note here that the selection of elastically scattered electrons around the diffraction spot increases the measured asymmetry of elastic scattering. In the inelastic part of the spectrum the intensity asymmetry even changes sign when we change selection from "inside" to "outside" the diffraction spot (compare b and c in Fig. 2). To find the radius R of the selection on the detector that contains only (mostly) diffracted electrons we analyzed the asymmetry of elastically scattered electrons as a function of the selection radius "r" at primary energy 14 eV. Fig. 3 represents such dependence. One can see that the absolute value of the asymmetry starts to decrease rapidly when the radius of the selection circle increases above 10 mm. Therefore we have chosen $R=10$ mm as the radius of the diffracted beam for all other primary energies from 8 eV to 27 eV.

3. Theoretical

In order to interpret our measured SPLEED asymmetry data and to supplement them by spin-dependent intensities we have carried out

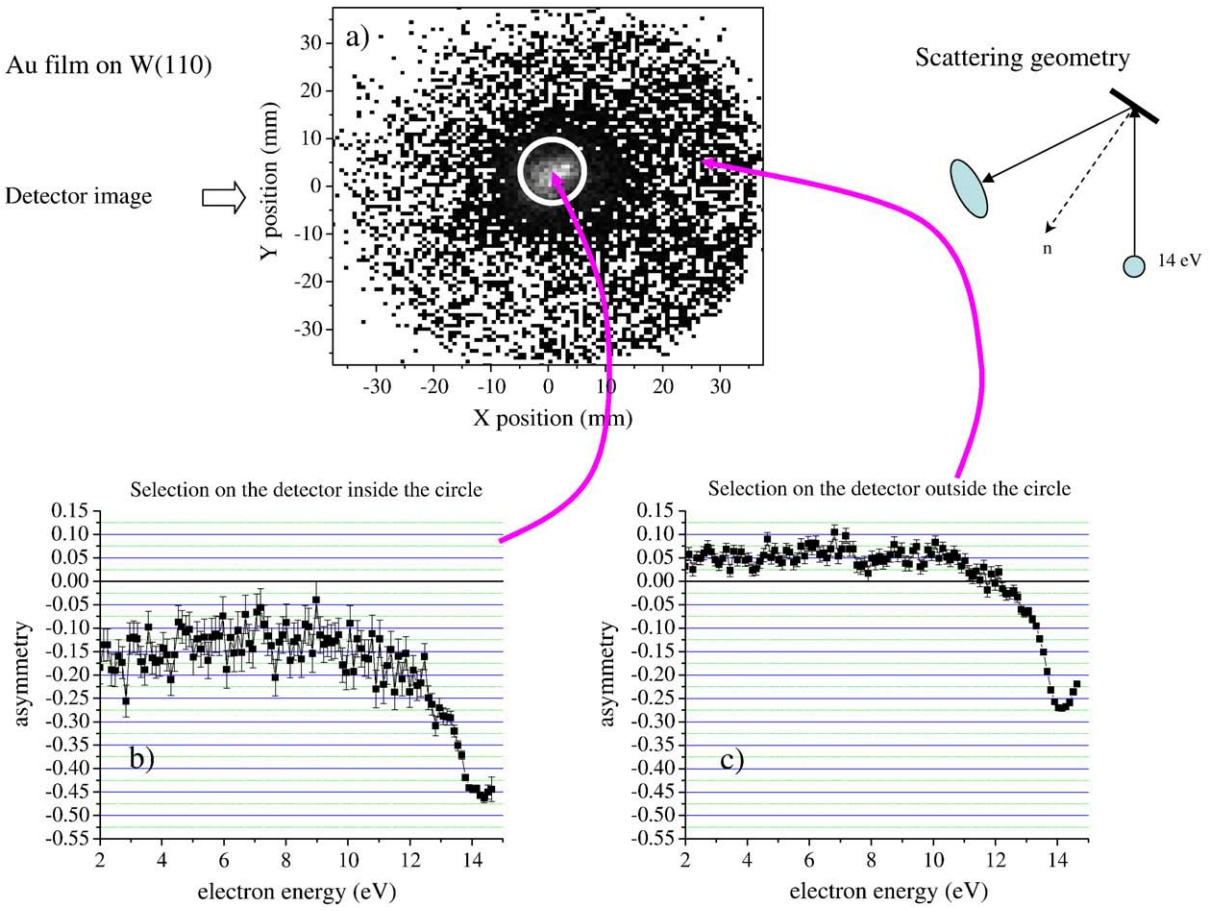

Fig. 2. Image of the diffraction spot on the detector (a); asymmetry of the secondary emission spectrum for electrons detected inside the circle shown on the detector (b); asymmetry measured outside of the white circle on the detectors (c).

corresponding SPLEED calculations using a relativistic layer-Korringa-Kohn-Rostoker (KKR) computer code. The underlying multiple-scattering formalism on the basis of the Dirac equation has been presented in detail earlier [1,23,24]. This formalism is equivalent to two other formalisms, which have also successfully been employed for SPLEED calculations ([25,26] and references therein).

Since our computer code requires two-dimensional periodicity, we performed the calculations for a semi-infinite Au(111), instead of a four-layer Au film which is incommensurate with the W(110) substrate. This appears reasonable due to the high surface sensitivity of SPLEED and due to the fact that the finite-size effects of the Au film (like e.g. the quantum-well resonances measured and calculated for Co films [27])do not play a role in the energy and angular ranges of our present work. The latter follows from SPLEED asymmetry measurements for varying film thickness, which will be discussed in the subsequent section of this paper

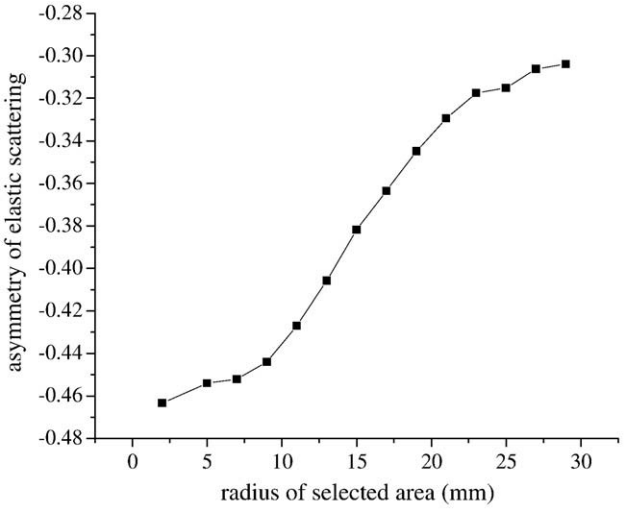

Fig. 3. Intensity asymmetry of elastically scattered electrons as a function of the selection radius on the detector.

The quasi-particle potential required for our SPLEED calculations consists of a real ground-state part and a complex self-energy correction. The ground-state part was obtained in a self-consistent density-functional theory calculation [24] using a local density approximation of the exchange-correlation potential [28]. The smooth surface potential barrier with image-potential asymptotics reproduces the features of the *L*-gap surface states of Au(111) [29]. Multiple scattering between this reflecting barrier and the topmost Au monatomic layer produces surface resonances just below the emergence thresholds of non-specular beams [30]. For comparison, we also performed calculations with a non-reflecting step barrier, for which surface resonances are absent.

We now address the complex self-energy correction to the ground-state potential. Its real part V_{re} has the effect of shifting electronic states and thence SPLEED spectra in energy. A value $V_{re} = 3$ eV was determined such as to optimize agreement between calculated and experimental spectra. This empirical choice implies that our V_{re} accounts not only for the actual real part of the self-energy but approximately also for the difference in the ground-state potentials, which pertain to the presently used local density approximation on the one hand and to the true non-local exchange-correlation functional on the other. Using a different approximation to

the exchange-correlation functional would therefore lead to practically the same SPLEED spectra.

For the imaginary part V_{im} of the self-energy correction, which accounts for inelastic scattering processes, we find that the parametrization $V_{im}(E) = 0.1\ (E - E_F)^{0.83}$, which proved successful for SPLEED from W(110) [15], also works well for the present case of Au(111). The effects of using a smaller or larger $V_{im}(E)$ will be addressed below in the context of the presentation of our SPLEED spectra.

Our calculated SPLEED quantities are the spin-dependent specular beam intensities I^+ and I^- for a primary beam of unit intensity and complete spin polarization parallel and antiparallel to the normal to the scattering plane. From these the asymmetry A is defined as:

$$A = \left(I^+ - I^-\right) / \left(I^+ + I^-\right) \tag{1}$$

and the figure of merit F_m for a spin detector as:

$$F_m = {}^1\!/_2 \cdot \left(I^+ + I^-\right) \cdot A^2. \tag{2}$$

4. Results and discussion

In Fig. 4 we compare the measured spin-asymmetry of the elastically scattered electrons (for polar angle of incidence 27°) as a function of the primary energy for clean W(110) [15] and 4 ML Au/W(110). The pronounced plus–minus feature for W(110) between 12 eV and 15 eV eV (i.e. +60% at about 13 eV and a sharp minimum of −30% at 14 eV) is seen to turn upon Au coverage into a minimum of −60% at about 14 eV. We note here that the measured asymmetry is normalized to the polarization of the incident beam (66%). The physical origin of the prominent asymmetry features in the two cases will be elucidated below by means of corresponding theoretical results.

To check whether finite-size effects (i.e. quantum-well resonances) contribute to our results, we performed measurements on Au films with thicknesses varying from 0 to about 5 monolayers (MLs). It turned out that the asymmetry minimum at 14 eV gets deeper with increasing film thickness: from about −30% for clean W(110) up to the saturation value of −60% reached for 2 ML Au/W(110). This finding rules out substantial contributions of quantum-well resonances for 4 ML Au/W(110) and lends support to comparing experimental results for the thin film system with theoretical ones obtained for semi-infinite Au(111), for which finite-size effects are necessarily absent.

In view of understanding our experimental Au asymmetry data (shown in Fig. 4), we present in Fig. 5 calculated spin-resolved intensities and asymmetries as functions of energy for Θ = 27°, calculated for two types of surface potential barriers: (i) a refracting non-reflecting and (ii) a reflecting smooth barrier (as described above in Section III). The intensities for the non-reflecting barrier (Fig. 5a) are seen to be fairly similar to those for the reflecting barrier (Fig. 5b), except that the latter exhibit pronounced surface resonance features just below 13 eV, which is the emergence threshold for a pair of non-specular beams. These resonances manifest themselves also in the asymmetry curve $A(E)$ (Fig. 5c) for the reflecting barrier. Most importantly, we note that for both barriers $A(E)$ exhibits a strong

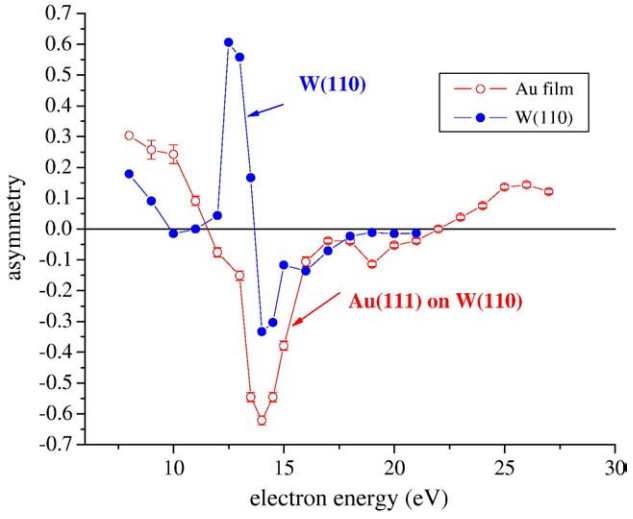

Fig. 4. Experimental asymmetries of (00) beams from W(110) (blue squares) and 4 ML Au/W(110) (red squares) versus energy. Angle of incidence = 27°. Asymmetries are normalized to an incident spin polarization of (66 ± 2%).

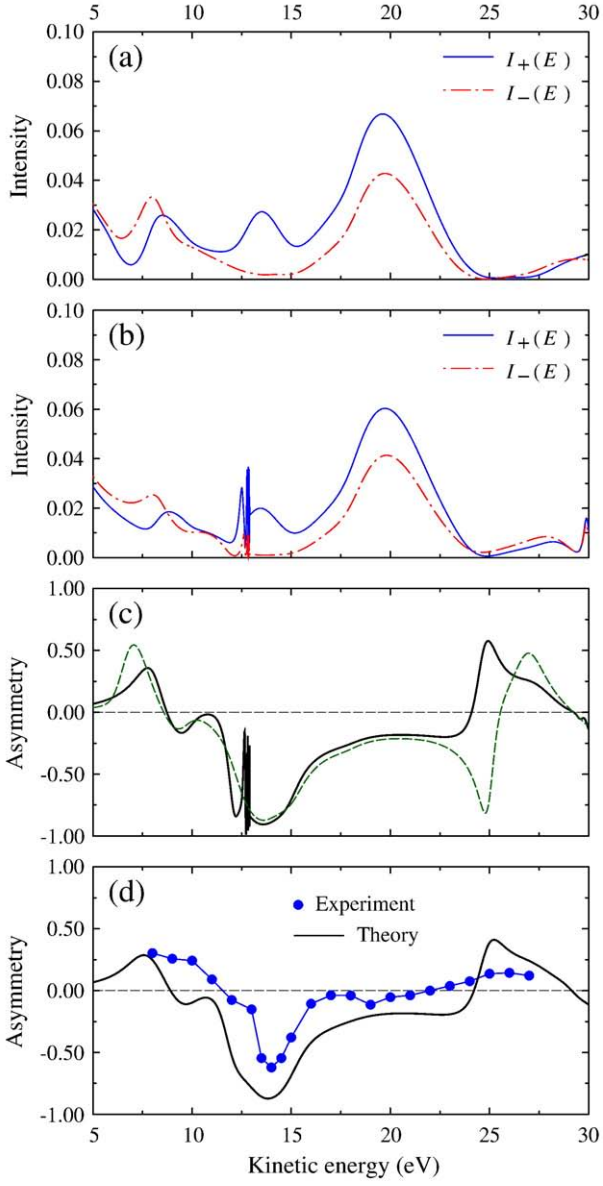

Fig. 5. SPLEED from Au/W(110) for theta = 27°. (a) Theoretical spin-resolved intensities versus energy for a non-reflecting surface barrier. (b) As in (a), but for a smooth (reflecting) surface barrier. (c) Theoretical asymmetries (cf. Eq. (1)) derived from the intensities shown in (a) (dashed green line) and in (b) (black solid line). (d) Comparison of experimental asymmetry (normalized to complete polarization of the incident beam) (blue dots) and theoretical one (solid line), which was obtained from the smooth barrier intensities convoluted by a Gaussian (width 0.5 eV) to mimic the experimental energy resolution.

minimum around 14 eV, where the intensities have a relative maximum. This asymmetry minimum is located slightly above the surface resonances. This is in contrast to the situation for W(110) (Fig. 4 and Ref. [15]), where a maximum in the asymmetry was observed in the energy range of the surfaces resonances. Consequently, details of the surface barrier are important for W, but not so for the present case of Au, where the asymmetry minimum essentially originates from the bulk-band structure with spin-orbit coupling.

In Fig. 5d we compare the experimental $A(E)$ curve (normalized to 66% degree polarization of the incident beam) with a theoretical one which has been obtained by convoluting the spin-resolved intensities for the smooth barrier with a Gaussian of width 0.5 eV. In particular the agreement in both shape and amplitude of the minimum supports that our theory captures the essential features of the experiment.

Since a potential source of uncertainty in the theoretical results lies in the assumed parametrization of the imaginary self-energy part V_{im}, we performed additional calculations with smaller and with larger V_{im}. While the intensity peaks get considerably narrower/broader with decreasing/increasing V_{im}, the overall effect on the asymmetry is comparatively small. For example, reducing/increasing V_{im} by 25% leads to only a few percent increase/reduction of the dominant minimum at 14 eV in the originally calculated asymmetry (in Fig. 5c) and even less in the convoluted asymmetry (in Fig. 5d).

To gain more information on the prominent minimum of $A(E)$ in Fig. 5d, we have measured and calculated the angular dependence of the asymmetry for the minimum energy 14 eV and two adjacent energies (13 and 15 eV). As can be seen in Fig. 6, both the theoretical and the experimental $A(\Theta)$ curves exhibit a broad minimum, which shifts towards higher angles when the energy decreases. The original (unconvoluted) theoretical $A(\Theta)$ curves further show that this minimum lies well above the sharp surface resonances. It is therefore – like the minimum in the $A(E)$ curves in Fig. 5 – of an essentially bulk-band-structure nature and hardly sensitive to the assumed surface-barrier potential model.

The above-shown agreement between experimental and theoretical asymmetries makes it most likely that our calculated intensities closely correspond to experimental intensities, which could not be measured with our present apparatus. We therefore now focus on theoretical results in search for conditions under which a high asymmetry A is associated with a high spin-averaged intensity I, since this implies a large figure of merit $F_m = I\,A^2$ for a potential spin polarimeter. In Fig. 7 we show – for a fixed angle of incidence 27° – spin-averaged intensity, asymmetry and figure-of-merit spectra. We note in particular that the large asymmetry feature around 14 eV coincides with a relative maximum in the intensity, leading to a large peak in the figure of merit. Its value of $7.5 \cdot 10^{-3}$ compares quite

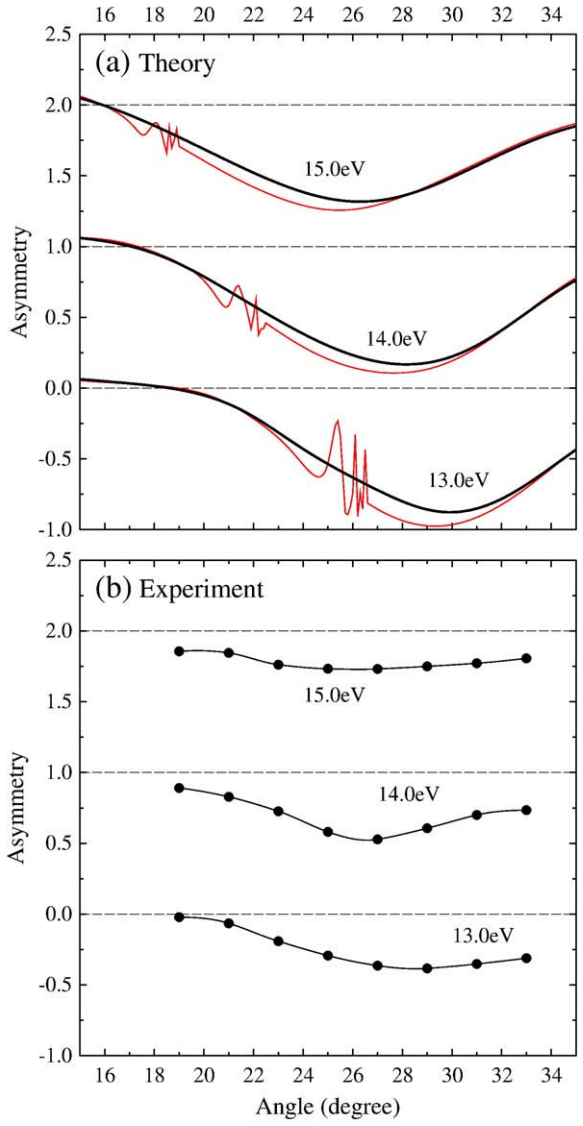

Fig. 6. Asymmetries versus angle of incidence for energies of 13 eV, 14 eV, and 15 eV. (a) Theoretical asymmetries for a smooth surface barrier, as calculated (thin red line) and convoluted by a Gaussian with a 2° width (thick black line). (b) Experimental asymmetries, normalized to complete spin polarization of the incident beam. Curves for 14 eV and 15 eV are shifted by 1 and 2 respectively along the ordinate.

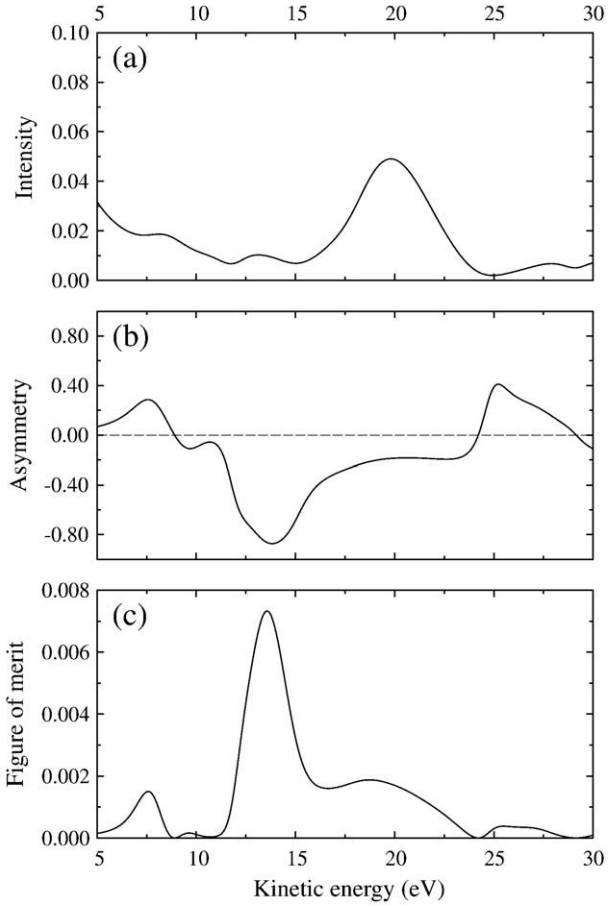

Fig. 7. Calculated specular-beam SPLEED spectra with a 0.5 eV Gaussian convolution from Au(111) for primary electrons incident at a polar angle of 27°. (a) Spin-averaged intensity $I(E)$ normalized to primary-beam intensity. (b) Asymmetry $A(E)$. (c) Figure of merit $F_m(E) = I(E)\,A(E)^2$.

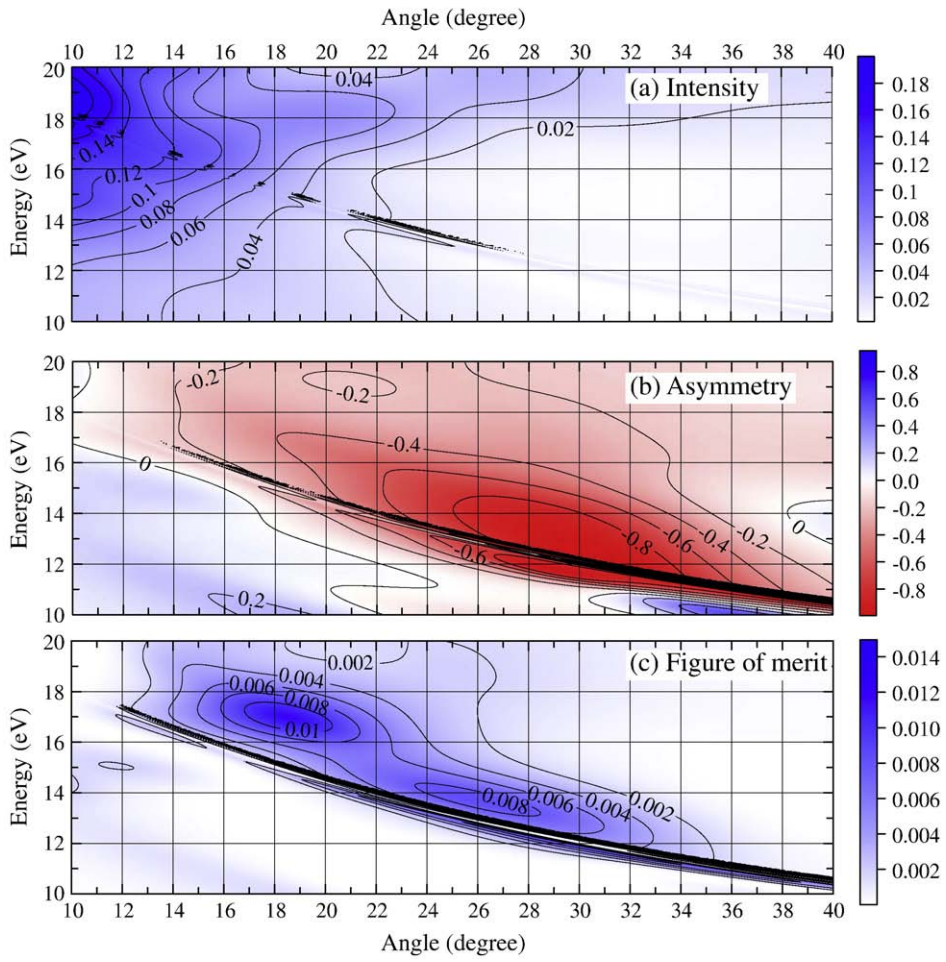

Fig. 8. Calculated specular-beam SPLEED from Au(111). Spin-averaged intensity (a), asymmetry (cf. Eq. (1)) (b), and figure of merit (cf. Eq. (2)) (c) as functions of energy E and polar angle θ of the primary beam.

favorably with the figures of merit of established spin detectors (cf. recent articles [5,6] and references therein).

To get a more comprehensive overview, we have explored a wider range of primary beam energies E and polar angles of incidence θ. The resulting spin-averaged intensity $I(E,\theta)$, asymmetry $A(E,\theta)$, and figure of merit $F_m(E,\theta)$ are shown as contour plots in Fig. 8. In Fig. 8b we note a fairly extended region of strong negative asymmetry which spans from 13 eV to 15 eV in energy and from 25 to 32° in angle. Although associated with only moderate intensities, it entails a high $F_m(E,\theta)$ plateau around (13.5 eV, 27°), as can be seen in Fig. 8c. This 'hot region' comprises the energies and angles, for which detailed results have been shown in Figs. 5–7. A further 'hot region' of F_m with even higher values (up to $1.5\cdot10^{-2}$) appears around $(E,\theta)=(17\text{ eV}, 19°)$.

In view of obtaining a practicable spin polarimeter, the following finding is important. The observed asymmetry spectra are very stable in time and resistant to contaminations. After 6 L exposure of the gold layer to oxygen (1 L = 1 s at 10^{-6} Torr) the value of asymmetry remains unchanged, in contrast to W(110) where the similar exposure to oxygen even changed the sign of asymmetry.

5. Conclusions

We have measured the intensity asymmetry of electrons elastically reflected from a Au film on W(110) surface for spin-polarized primary electrons with energy from 8 to 27 eV. In particular, we observed an asymmetry-versus-energy spectrum which is dominated by a large feature of about −60% slightly above the emergence threshold for non-specular beams.

In order to understand our experimental data, we calculated spin-dependent LEED intensity spectra and the corresponding spin-asymmetry spectra by means of a relativistic multiple-scattering formalism. We obtained agreement with our experimental asymmetry curves.

The occurrence of strong spin-asymmetries in SPLEED also has implications for designing or interpreting spin-resolved photoemission and $(e,2e)$ experiments, in which the final state consists of one or two time-reversed LEED states. Further, we would like to mention a potential relevance of our results for spintronics. Finally, we emphasize that for a fairly extended energy and angular range we found a very high figure of merit, which promises an application for a very efficient new spin polarimeter.

Acknowledgments

This research was supported by the Australian Research Council and the University of Western Australia. We thank S. Key, G. Light and A. Sergeant (UWA) for their help in preparation of experiments.

References

[1] J. Kessler, Polarized Electrons, Springer, Berlin, 1985.
[2] R. Feder (Ed.), Polarized Electrons in Surface Physics, World Scientific, Singapore, 1985.
[3] J. Kirschner, Polarized Electrons at Surfaces, Springer, London, 1985.
[4] V.N. Petrov, V.V. Grebenshikov, B.D. Grachev, A.S. Kamochkin, Rev. Sci. Instrum. 74 (2003) 1278.
[5] A. Winkelmann, D. Hartung, H. Engelhard, C.-T. Chiang, J. Kirschner, Rev. Sci. Instrum. 79 (2008) 083303.

[6] T. Okuda, Y. Takeichi, Y. Maeda, A. Harasawa, I. Matsuda, T. Kinoshita, A. Kakizaki, Rev. Sci. Instrum. 79 (2008) 123117.
[7] R. Feder, Surf. Sci. 68 (1977) 229.
[8] N. Fominykh, J. Henk, J. Berakdar, P. Bruno, Surf. Sci. 507–510 (2002) 229.
[9] S. LaShell, B.A. McGougall, E. Jensen, Phys. Rev. Lett. 77 (1996) 3419.
[10] G. Nicolay, F. Reinert, S. Hüfner, P. Blaha, Phys. Rev. B 65 (2001) 033407.
[11] M. Hoesch, M. Muntwiler, V.N. Petrov, M. Hengsberger, L. Patthey, M. Shi, M. Falub, T. Greber, J. Osterwalder, Phys. Rev. B 69 (2004) 241401(R).
[12] M. Muntwiler, M. Hoesch, V.N. Petrov, M. Hengsberger, L. Patthey, M. Shi, M. Falub, Th. Greber, J. Osterwalder, J. Electron. Spectrosc. Relat. Phenom. 137–140 (2004) 119.
[13] J. Henk, A. Ernst, P. Bruno, Phys. Rev. B 68 (2003) 165416.
[14] P.D. Augustus, J.P. Jones, Surf. Sci. 64 (1977) 713.
[15] S.N. Samarin, J.F. Williams, A.D. Sergeant, O.M. Artamonov, H. Gollisch, R. Feder, Phys. Rev. B 76 (2007) 125402.
[16] J. Henk, M. Hoesch, J. Osterwalder, A. Ernst, P. Bruno, J. Phys. Condens. Matter 16 (2004) 7581.
[17] R. Cortenraada, S.N. Ermolov, V.N. Semenov, A.W. Denier van der Gon, V.G. Glebovsky, S.I. Bozhko, H.H. Brongersma, J. Cryst. Growth 222 (2001) 154.
[18] S. Samarin, J. Berakdar, R. Herrmann, H. Schwabe, O. Artamonov, J. Kirschner, J. Phys. IV France 9 (1999) Pr6-137-Pr6-143.
[19] H. Knoppe, E. Bauer, Phys. Rev. B 48 (1993) 5621.
[20] A.M. Shikin, O. Rader, G.V. Prudnikova, V.K. Adamchuk, W. Gudat, Phys. Rev. B 65 (2002) 075403.
[21] S.N. Samarin, O.M. Artamonov, D.K. Waterhouse, J. Kirschner, A. Morozov, J.F. Williams, Rev. Sci. Instrum. 74 (2003) 1274.
[22] D.T. Pierce, R.J. Celotta, G.-C. Wang, W.N. Unertl, A. Galejs, C.E. Kuyatt, S.R. Mielczarek, Rev. Sci. Instrum. 51 (1980) 478.
[23] S.V. Halilov, E. Tamura, H. Gollisch, D. Meinert, R. Feder, J. Phys. Condens. Matter 5 (1993) 3859.
[24] J. Henk, in: H.S. Nalwa (Ed.), Handbook of Thin Film Materials, vol. 2, Academic Press, San Diego, 2002, p. 479.
[25] R.O. Jones, P.J. Jennings, Surf. Sci. Rep. 9 (1988) 165.
[26] H. Tang, M. Plihal, D.L. Mills, Phys. Rev. B 54 (1996) 14172.
[27] T. Scheunemann, R. Feder, J. Henk, E. Bauer, T. Duden, H. Pinkvos, H. Poppa, K. Wurm, Solid State Commun. 104 (1997) 787.
[28] J.P. Perdew, Y. Wang, Phys. Rev. B. 45 (1992) 13244.
[29] J. Henk, W. Schattke, H. Carstensen, R. Manzke, M. Skibowski, Phys. Rev. B 47 (1993) 2251.
[30] E.G. McRae, Rev. Mod. Phys. 51 (1979) 541.